

Organic & Biomolecular Chemistry

Accepted Manuscript



This is an *Accepted Manuscript*, which has been through the Royal Society of Chemistry peer review process and has been accepted for publication.

Accepted Manuscripts are published online shortly after acceptance, before technical editing, formatting and proof reading. Using this free service, authors can make their results available to the community, in citable form, before we publish the edited article. We will replace this *Accepted Manuscript* with the edited and formatted *Advance Article* as soon as it is available.

You can find more information about *Accepted Manuscripts* in the [Information for Authors](#).

Please note that technical editing may introduce minor changes to the text and/or graphics, which may alter content. The journal's standard [Terms & Conditions](#) and the [Ethical guidelines](#) still apply. In no event shall the Royal Society of Chemistry be held responsible for any errors or omissions in this *Accepted Manuscript* or any consequences arising from the use of any information it contains.

Multivalency effects in *Pseudomonas aeruginosa* biofilm inhibition and dispersal by glycopeptide dendrimers targeting lectin LecA

Myriam Bergmann,^{a)} Gaëlle Michaud,^{a)} Ricardo Visini,^{a)} Xian Jin,^{a)} Emilie Gillon,^{b)} Achim Stocker,^{a)} Anne Imberty,^{b)} Tamis Darbre*^{a)} and Jean-Louis Reymond^{a)*}

^{a)} Department of Chemistry and Biochemistry, University of Berne, Freiestrasse 3, 3012 Berne Switzerland. FAX: + 41 31 631 80 57. e-mail: jean-louis.reymond@dcb.unibe.ch ^{b)} Centre de Recherches sur les Macromolécules Végétales, UPR5301, CNRS and Université Grenoble Alpes, 601 rue de la Chimie, F38041 Grenoble, France

Abstract

The galactose specific lectin LecA partly mediates the formation of antibiotic resistant biofilms by *Pseudomonas aeruginosa*, an opportunistic pathogen causing lethal airways infections in immunocompromised and cystic fibrosis patients, suggesting that preventing LecA binding to natural saccharides might open new opportunities for treatment. Here 8-fold (G3) and 16-fold (G4) galactosylated analogs of **GalAG2**, a tetravalent G2 glycopeptide dendrimer LecA ligand and *P. aeruginosa* biofilm inhibitor, were obtained by convergent chloroacetyl thioether (ClAc) ligation between 4-fold or 8-fold chloroacetylated dendrimer cores and digalactosylated dendritic arms. Hemagglutination inhibition, isothermal titration calorimetry and biofilm inhibition assays showed that G3 dendrimers bind LecA slightly better than their parent G2 dendrimers and induce complete biofilm inhibition and dispersal of *P. aeruginosa* biofilms, while G4 dendrimers show reduced binding and no biofilm inhibition. A binding model accounting for the observed saturation of glycopeptide dendrimer galactosyl groups and LecA binding sites is proposed based on the crystal structure of a G3 dendrimer LecA complex.

Introduction

Pseudomonas aeruginosa is an opportunistic gram negative human pathogen causing lethal airways infections in immunocompromised and cystic fibrosis patients by forming antibiotic resistant biofilms.¹ One of the therapeutic approaches to fight these infections consists in developing biofilm inhibitors to restore antibiotic sensitivity with reduced effect in the resistance phenomena.² It has been shown that tissue attachment and biofilm formation in *P. aeruginosa* is mediated in part by the galactose specific lectin LecA (PA-IL)³ and the fucose specific lectin LecB (PA-IIL),⁴ as evidenced by the impaired biofilm formation in deletion mutants⁵ and case reports of treating *P. aeruginosa* infections using lectin-binding saccharide solutions,⁶ leading to the hypothesis that targeted inhibitors of these lectins might allow to control biofilms.⁷

Following this hypothesis ligands of LecA,⁸ LecB,⁸ or both,⁹ have been reported featuring various monovalent or multivalent glycosides displayed on a multivalent scaffold.¹⁰ However only very few examples were reported to actually interfere with *Pseudomonas aeruginosa* biofilm formation.¹¹ In particular we recently reported glycopeptide dendrimers displaying four α -L-C-fucoside groups (**FD2**: (Fuc- α -CH₂CO-Lys-Pro-Leu)₄(Lys-Phe-Lys-Ile)₂Lys-His-Ile-NH₂)¹² or analogs with four galactoside groups (**GalAG2**: (Gal- β -OC₆H₄CO-Lys-Pro-Leu)₄(Lys-Phe-Lys-Ile)₂Lys-His-Ile-NH₂; **GalBG2**: (Gal- β -S-CH₂CH₂CO-Lys-Pro-Leu)₄(Lys-Phe-Lys-Ile)₂Lys-His-Ile-NH₂)¹³ at the end of a common second generation (G2) peptide dendrimer scaffold.¹⁴ These dendrimers bound tightly to their respective lectin, and inhibited the formation and induced partial dispersion of *P. aeruginosa* biofilms, representing an interesting example of bioactive synthetic dendrimers.¹⁵

Tight lectin binding and biofilm inhibition by these tetravalent G2 dendrimers depended on a multivalency effect since the lower generation analogs (G0 and G1) were essentially inactive.¹⁶ In the case of the **GalAG2** lectin binding was enhanced by a specific CH- π interaction between the

(ϵ)-CH of His50 on LecA and the aromatic ring of the GalA aglycone leading to further binding interactions between the terminal tripeptide arm of the dendrimer and LecA, however optimization of the amino acid sequence of this tripeptide only resulted in modest activity improvements.¹⁷ Considering that many of the reported high affinity multivalent glycosidic ligands for lectins feature an 8-fold or higher multivalency, we asked the question whether the binding affinity and biological activity of dendrimers **GalAG2** and **GalBG2** might be increased in higher valency analogs as observed in other series of tight binding LecA ligands.⁸ Various G3 and G4 analogs of **GalAG2** and **GalBG2** were prepared using the multiple chloroacetyl cysteine (ClAc) thioether ligation as the key step.¹⁸ Hemagglutination inhibition, isothermal titration calorimetry and biofilm inhibition assays are reported that show that G3 dendrimers bind LecA slightly better than their parent G2 dendrimers and induce complete biofilm inhibition and dispersal of *P. aeruginosa* biofilms, while G4 dendrimers have reduced binding and no biofilm inhibition. A binding model accounting for the observed saturation of glycopeptide dendrimer galactosyl groups and LecA binding sites is proposed based on a crystal structure of a G3 dendrimer LecA complex.

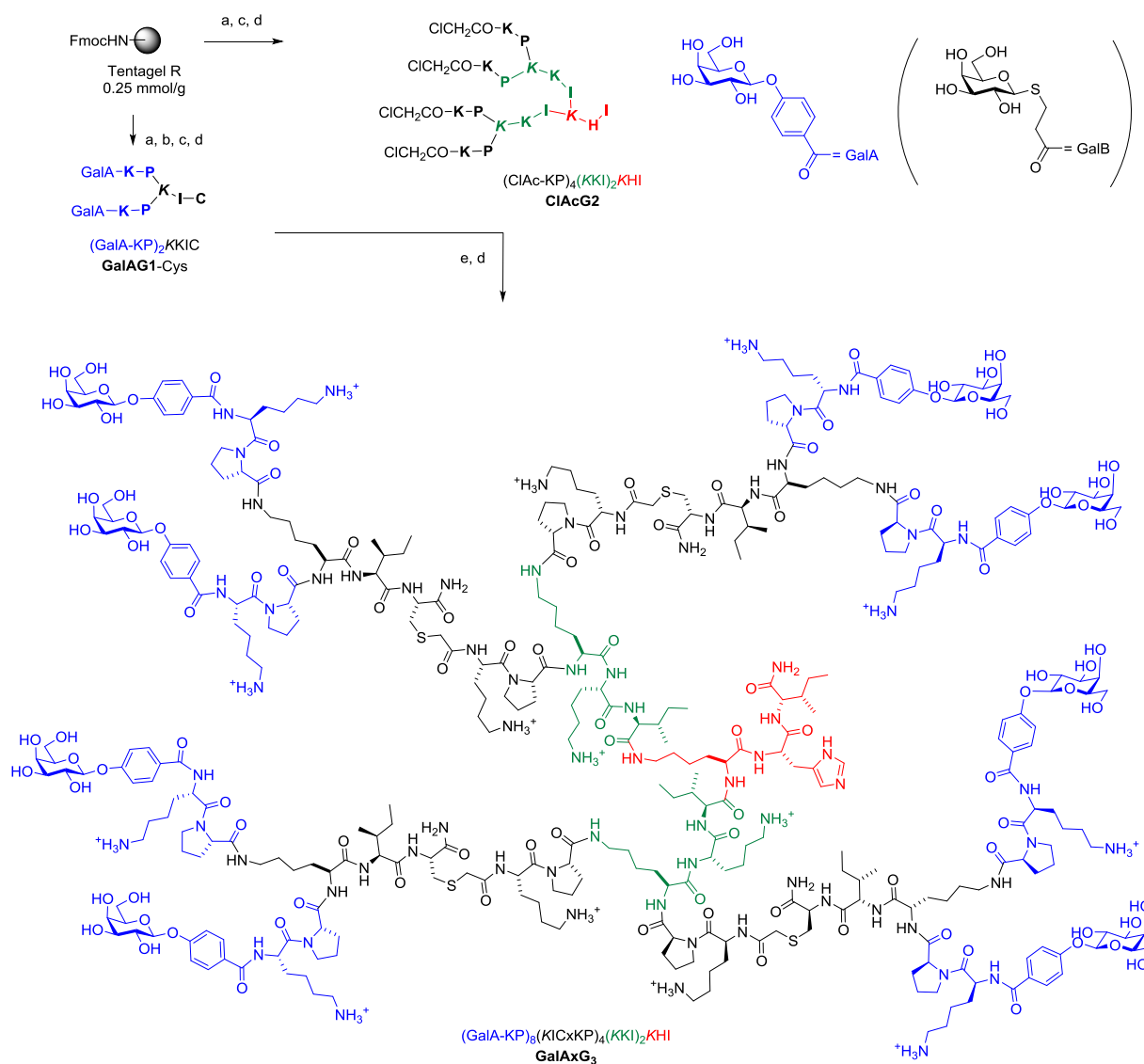


Figure 1. Convergent synthesis and structural formula of the octavalent G3 glycopeptide dendrimer **GalAxG3** with the corresponding sequence notation. Sequences are written with N-terminus at left and C-terminus at right, the C-terminus of the peptide are carboxamide (CONH₂). One letter codes are used for standard amino acids, the branching diamino acid lysine is in italics and extended on both amino groups, x = -S-CH₂-CO-. The detailed structure of the terminal galactosides abbreviated GalA and GalB in the abbreviated sequence notation of the dendrimers used in Table 1 and 2 are shown at top right. Conditions: a) SPPS: Fmoc deprotection with piperidine/DMF 1:4 (v/v), 2x15 min.; Amino acid coupling (3 eq. Fmoc-aa-OH, 3 eq. PyBOP, 5 eq. DIEA in NMP), 2-4 hours; carbohydrate coupling: 4 eq. Ac₄GalA-OH, 3 eq. HCTU, 5 eq. DIPEA in NMP, overnight; b) Deacetylation: MeOH/25% NH₃/H₂O (8:1:1, v/v/v); c) Cleavage: TFA/TIS/H₂O (95:2.5:2.5, v/v/v); d) RP-HPLC purification; e) ClAc ligation: **ClAcG2** (1 eq.), **GalAG1-Cys** (6 eq.), KI (20 eq.) DIPEA (55 eq.) in DMF/H₂O (1:1, v/v), RT, overnight under Argon atmosphere.

Results and Discussion

Synthesis

Although we previously reported a single case of a G3 glycopeptide dendrimer by direct SPPS,^{12c} the synthesis was difficult and the isolated yield was very low due to incomplete coupling of the glycosidic end group to the multiple *N*-termini even with low loading resin (~0.2 mmol/g) and large excess of glycosylated reagent. This is probably a result of the steric crowding in the G3 dendrimer with some of the amino termini not exposed to the coupling reagents. This step proved to be a limiting factor across various peptide dendrimers and carbohydrate building blocks even for G2 peptide dendrimers despite the fact that the reaction is a standard amide bond formation step. We therefore turned our attention to a convergent approach using our recently reported multivalent ClAc ligation method as an efficient strategy to access G3 and G4 peptide dendrimers (Figure 1).¹⁸

SPPS was first used to prepare a G1 glycopeptide dendrimer featuring the *N*-terminal dipeptide LysPro of **GalAG2** known to engage in direct contact with the lectin, which was acylated at its two *N*-termini with either 4-carboxyphenyl- β -galactoside to yield **GalAG1-Cys** or carboxypropyl- β -thiogalactoside to yield **GalBG1-Cys**. The carbohydrate building block coupling step was not problematic at the G1 level and both products were obtained in good yield after purification by preparative HPLC. The amino acid sequence of **GalAG2** was then used to design the 2-fold, 4-fold and 8-fold chloroacetylated core dendrimers **ClAcG1**, **ClAcG2** and **ClAcG3** consisting of dipeptide branches. The chloroacetylated dendrimer cores **ClAcPSG2** and **ClAcPSG3** were also prepared since they were found previously to give high yields in ClAc ligation reactions.¹⁸ Isolated yields of these various chloroacetylated core dendrimers after SPPS and HPLC purification were above 25 % for G1 and G2, but only 3-5 % for the G3 cores, reflecting the generally more difficult synthesis of G3 peptide dendrimers (Table 1).

The ClAc ligation was then performed to append to different dendrimer cores multiple copies of the **GalAG1-Cys** dendrimer bearing a phenyl- β -galactoside LecA ligand. Dendrimers **ClAcG1** and **ClAcG2** were also ligated to **GalBG1-Cys** to obtain G2 and G3 analogs with a thiopropyl- β -galactoside endgroup. The ligation reactions generally proceeded cleanly and gave isolated yields in the range 64-80%, except for **GalAxG4** which was obtained in only 12% yield due to a difficult purification.

Table 1. Convergent synthesis of glycopeptide dendrimers using the multivalent ClAc ligation.

Name	Sequence ^{a)}	MS calc./obs. ^{b)}	Yield mg (%) ^{c)}
Components from SPPS			
GalAG1-Cys	(GalA-KP) ₂ KIC	1376.6/1377	63 (41.6%)
GalBG1-Cys	(GalB-KP) ₂ KIC	1312.6/1312.6	57 (39.5%)
ClAcG1	(ClAc-KI) ₂ KHI	1031.1 /1030	41.4 (36.55%)
ClAcG2	(ClAc-KP) ₄ (KKI) ₂ KHI	2341.6/2341	64 (25%)
ClAcG3	(ClAc-KP) ₈ (KLF) ₄ (KKI) ₂ KHI	5102.7/5102	19.3 (3.4%)
ClAcPSG2	(ClAc-PS) ₄ (KPS) ₂ KPS	1996.8/1996.9	66 (30%)
ClAcPSG3	(ClAc-PS) ₈ (KPS) ₄ (KPS) ₂ KPS	4289/4290	25 (5%)
GalAPSG2	(GalA-KPL) ₄ (KPS) ₂ KPS	3437.9/3478	26.4 (6%)
Dendrimers prepared by ClAc ligation			
GalAxG2	(GalA-KP) ₄ (KICxKI) ₂ KHI	3711.3/3711	6.9 (64%)
GalAxG3	(GalA-KP) ₈ (KICxKP) ₄ (KKI) ₂ KHI	7702/7701	7.3 (70%)
GalAxG4	(GalA-KP) ₁₆ (KICxKP) ₈ (KLF) ₄ (KKI) ₂ KHI	15823.6/15825	1.1 (12%)
GalAxPSG3	(GalA-KP) ₈ (KICxPS) ₄ (KPS) ₂ KPS	7357.3/7358	9.7 (74.5%)
GalAxPSG4	(GalA-KP) ₁₆ (KICxPS) ₈ (KPS) ₄ (KPS) ₂ KPS	15009.9/15010.6	9.1 (80.8%)
GalBxG2	(GalB-KP) ₄ (KICxKI) ₂ KHI	3583.4/3582.7	6.7 (64.5%)
GalBxG3	(GalB-KP) ₈ (KICxKP) ₄ (KKI) ₂ KHI	7446.2/7445	6.2 (64%)

^{a)} Sequence notation for peptide dendrimers using single letter amino acid codes for L-amino acids and indicating the branching lysine in italics. See Figure 1 for the correspondence between sequence notation and complete structural formula, illustrated for dendrimer **GalAxG3**. Further abbreviations: ClAc = ClCH₂CO-, x = -CH₂SCH₂CO-, GalA = 4-(β -galactosyloxy)benzoyl, GalB = (β -galactosyl)SCH₂CH₂CO-, the peptide C-terminus is carboxamide (CONH₂). ^{b)} ESI+ or MALDI. ^{c)} yields are for purified compounds after SPPS (upper part) or ClAc ligation (lower part) and preparative HPLC.

Hemagglutination inhibition assays

Binding of the various glycopeptide dendrimers to lectin lecA was first investigated in a hemagglutination inhibition assay (Table 2, left part). In this assay compounds are tested in two-fold dilution series for their inhibition of the agglutination of erythrocytes induced by the lectin, providing minimal hemagglutination inhibition concentration (MIC) values. The MIC values are then scaled to the reference MIC value of free galactose in each assay to yield relative potencies (r.p.) of inhibition. Although absolute MIC values of both test compounds and the reference galactose may vary depending on erythrocyte source and lectin concentration, r.p. values are quite

reproducible and a good indicator of multivalent binding potential. Here the primary r.p. values were further converted to secondary r.p. value by scaling to the r.p. of the parent monovalent glycopeptides **GalAG0** and **GalBG0** as reference. This allowed quantifying multivalency effects independently of affinity effects on monovalent ligand binding. These effects were quite substantial in the case of **GalAG0**, which inhibits hemagglutination at a 40-fold lower concentration than free D-galactose. A similar effect also occurs with *p*-nitrophenyl- β -galactoside and reflects a productive CH- π interaction of the aromatic aglycone with the C(ϵ)-H of His55 on the lectin.¹⁷ The r.p. values were furthermore scaled to the number of galactosyl endgroup (n_{Gal}) to correct for multivalency.

In the phenyl-galactoside (GalA) series there was no significant increase in r.p./ n_{Gal} in the divalent dendrimer **GalAG1**, but the tetravalent dendrimer **GalAG2** was 26-fold stronger than **GalAG0** on a per galactose basis. A comparable multivalency effect was obtained with the tetravalent ClAc analog **GalAxG2** (r.p./ n_{Gal} = 31), showing that the modification of the peptide dendrimer backbone performed to enable the convergent ClAc ligation did not influence hemagglutination inhibition significantly. Increasing dendrimer size to octavalency resulted in a more modest, 4-fold increase in relative potency per galactosyl endgroup with **GalAxG3** (r.p./ n_{Gal} = 125), respectively 14-fold increase in its analog **GalAxPSG3** (r.p./ n_{Gal} = 375). However there was no further increase in relative potency at the G4 level, with the 16-valent **GalAxG4** (r.p./ n_{Gal} = 50) showing a 2.5-fold drop and **GalAxPSG4** (r.p./ n_{Gal} = 475) a 1.3-fold increase in potency relative to the corresponding G3 dendrimers. In the thiopropyl-galactoside (GalB) series multivalency effects in hemagglutination inhibition were much weaker, with r.p./ n_{Gal} values increasing only up to 8-fold in **GalBxG3**.

Isothermal titration calorimetry (ITC)

Multivalency effects in the dendrimer LecA interactions were also investigated by ITC using *p*-nitrophenyl- β -galactoside (K_{D} = 16 μM) as reference. Binding enthalpies ΔH and dissociation constants K_{D} were determined experimentally by titrating the various ligands into a LecA solution,

and used to calculate binding entropies ΔS and binding free energies ΔG (Table 2, right part, and supporting information Figure S47). The binding enthalpy ΔH amounted to approximately 14 kcal/mol per galactosyl end group across all ligands tested. The GalA ligands showed generally stronger binding compared to the corresponding GalB ligands, implying a smaller entropic penalty on binding consistent with their more rigid structure and the burial of a larger hydrophobic surface area upon lectin binding. The percentage of bound galactose per dendrimer was also obtained, a value which was somewhat imprecise due to small errors in concentration determination caused by varying amounts of water in the lyophilized powders of the purified dendrimers. Values $> 80\%$ were interpreted as complete engagement of all dendrimer galactosyl groups with the lectin, with incomplete binding observed only in the case of the G4 dendrimer **GalAPSG4** (40 % bound galactose).

In each series the multivalency effect on binding was quantified by the relative potency of binding per galactosyl endgroup (r.p./n_{Gal}), which was calculated from the ratio between the K_D of the reference monovalent glycotriptide ligand **GalAG0** or **GalBG0** and the K_D of the multivalent dendrimer. In the GalA series the relative potency increase in the G0/G1/G2 series (1/18/296) was much stronger than that observed in the hemagglutination assay (1/1.3/26). A further 1.4-fold increase in relative potency occurred in the homologous ClAc synthesis series **GalAxG2/GalAxG3** (107/148), although both compounds were less potent than the parent **GalAG2** dendrimer. Further generation increase was detrimental to binding, as evidenced by a relative potency decrease by 1.6-fold in the sequence **GalAxPSG3/GalAxPSG4** (88/54). In the GalB series the relative potency increase in the G0/G1/G2 series (1/18/230) was comparable to that observed with the GalA series, in particular with a 13-fold increase in relative potency when moving from the divalent G1 dendrimer to the tetravalent G2 dendrimer, which was comparable to the 16-fold increase observed in the GalA series. As for the GalA series the gain in relative potency was much smaller between tetravalent G2 and octavalent G3 GalB type dendrimers and amounted to only 2.8-fold (280/785).

Taken together, the ITC data confirmed hemagglutination inhibition assays in showing that, while a very strong multivalency effect occurred at the level of the tetravalent G2 dendrimers, only a relatively modest increase in relative potency per galactosyl endgroup (1.4 to 4-fold) was possible by moving to higher multivalency dendrimers. It should be noted that ITC might not be able to measure K_D values below 1nM and might therefore obscure an increase in potency in the relatively tight binding GalA series. Nevertheless this uncertainty should not affect the results in the weaker binding GalB series reaching to $K_D = 5.9$ nM for **GalBxG3** reflecting a 2.8-fold increase in relative potency per galactosyl group compared to its G2 analog.

Table 2. Hemagglutination assay and isothermal titration calorimetry data for *P. aeruginosa* LecA binding.

Ligand	Sequence ^{a)}	Hemagglutination assay ^{b)}				Isothermal titration calorimetry (ITC) ^{c)}						
		n _{Gal}	MIC μM	r.p./n	N	% bnd Gal	ΔH [kcal/mol]	-TΔS	ΔG	K _D [nM]	r.p./n _{Gal}	
D-Galactose		1	42000 (3125*)	-	-	-	-	-	-	-	-	-
NPG	<i>p</i> -Nitrophenyl-β-galactoside	1	-	-	0.91 ± 0.03	-	-10.6 ± 0.5	4.04	6.53	16000 ± 500	-	-
IPTG	Isopropyl-β-thiogalactoside	1	10400	-	-	-	-	-	-	-	-	-
GalAG0	(GalA-KPL)	1	80*	1	0.65 ± 0.02	100	-17.8 ± 0.3	10.2	-7.5	2960 ± 50	1	1
GalAG1	(GalA-KPL) ₂ KHI	2	31*	1.3	0.302 ± 0.003	93	-29 ± 0.5	19.3	-9.7	83 ± 12	18	18
GalAG2	(GalA-KPL) ₄ (KFKI) ₂ KHI	4	0.78*	26	0.136 ± 0.001	84	-69 ± 1.1	57	-11.7	2.5 ± 0.1	296	296
GalAxG2	(GalA-KP) ₄ (KICxKI) ₂ KHI	4	8.3	31	0.16 ± 0.009	98	-54 ± 1	43	-11.1	6.9 ± 1.4	107	107
GalAxG3	(GalA-KP) ₈ (KICxKP) ₄ (KKI) ₂ KHI	8	1.04	125	0.064 ± 0.01	79	-115 ± 8	103.0	-11.7	2.5 ± 0.2	148	148
GalAxG4	(GalAKP) ₁₆ (KICxKP) ₈ (KLF) ₄ (KKI) ₂ KHI	16	1.28	50	-	-	-	-	-	-	-	-
GalAPSG2	(GalA-KPL) ₄ (KPS) ₂ KPS	4	0.78	40	-	-	-	-	-	-	-	-
GalAxPSG3	(GalA-KP) ₈ (KICxPS) ₄ (KPS) ₂ KPS	8	0.35	375	0.096 ± 0.001	>100	-92 ± 0.5	81	-11.4	4.2 ± 0.2	88	88
GalAxPSG4	(GalAKP) ₁₆ (KICxPS) ₈ (KPS) ₄ (KPS) ₂ KPS	16	0.14	475	0.033 ± 0.001	41	-217 ± 17	206	-11.5	3.4 ± 0.4	54	54
GalBG0	(GalB-KPL)	1	2500*	1	0.71 ± 0.01	100	-14 ± 0.04	7.8	-6.0	37000 ± 800	1	1
GalBG1	(GalB-KPL) ₂ KHI	2	630*	1.9	0.37 ± 0.02	>100	-20 ± 0.1	12	-8.2	1060 ± 160	18	18
GalBG2	(GalB-KPL) ₄ (KFKI) ₂ KHI	4	125*	4.8	0.18 ± 0.02	>100	-43 ± 1	33	-10.1	40 ± 1	230	230
GalBxG2	(GalB-KP) ₄ (KICxKI) ₂ KHI	4	125*	4.8	0.14 ± 0.001	79	-47 ± 6	37	-11.2	33 ± 25	280	280
GalBxG3	(GalB-KP) ₈ (KICxKP) ₄ (KKI) ₂ KHI	8	37.5*	8.3	0.08 ± 0.01	90	-90 ± 9	79	-11.4	5.9 ± 2	785	785

^{a)} Sequence notation for peptide dendrimers using single letter amino acid codes for L-amino acids and indicating the branching lysine in italics. See Figure 1 for the correspondence between sequence notation and complete structural formula, illustrated for dendrimer **GalAxG3**. Further abbreviations: GalA = 4-(β-galactosyloxy)benzoyl, GalB = (β-galactosyl)SCH₂CH₂CO, x = -CH₂SCH₂CO-, the peptide C-terminus is carboxamide (CONH₂). ^{b)} Minimal hemagglutination inhibition concentrations (MIC) were determined in two different series with the MIC for galactose was 42 mM or 3.125 mM, marked with *, n_{Gal} is the number of galactosyl groups per compound, r.p./n is the relative potency per galactosyl group relative to free galactose as reference: MIC(galactose)/(n×MIC(compound)), r.p./nGalA or B is the relative potency per galactosyl group relative to GalAG0 or GalBG0 as reference: MIC(GalAG0 or GalBG0)/(n×MIC(compound)) ^{c)} Thermodynamic parameters and dissociation constants K_D are reported as an average of two independent runs from ITC in 20 mM Tris, 100 mM NaCl, 100 μM CaCl₂, pH=7.5. Titration concentrations (Ligand/LecA) are the following: NPG (3 mM/0.3 mM), **GalAG0** (0.5 mM/0.0516 mM), **GalAG1** (0.25 mM/0.0486 mM), **GalAG2** (0.03 mM/0.018 mM), **GalAxG2** (0.03 mM/0.016 mM), **GalAxG3** (0.015 mM/0.017 mM), **GalAxG3PS** (0.015 mM/0.0146 mM), **GalAxG4PS** (0.01 mM/0.019 mM), **GalBG0** (1.0 mM/0.091 mM), **GalBG1** (0.25 mM/0.049 mM), **GalBG2** (0.03 mM/0.018 mM), **GalBxG2** (0.03 mM/0.021 mM), **GalBxG3** (0.015 mM/0.013 mM). N = stoichiometry value in ligand / galactose binding site on LecA. r.p./n_{Gal} = relative potency per galactosyl group relative to the parent monovalent ligand **GalAG0** or **GalBG0**.

Biofilm inhibition

P. aeruginosa biofilms were induced by growing the bacteria in 0.25% (w/v) nutrient broth No.2, Oxoid, medium in 96-well sterile, U-bottomed polystyrene microtiter plates. Biofilm inhibition was determined by quantifying the amount of biofilm formed after 24 h of growth in the presence or absence of glycodendrimers or control compounds at different concentrations. The biofilm was quantified using the WST-8 assay indicating the amount of viable cells,¹⁹ rather than with the crystal violet assay indicating the overall biomass.^{19b, 19c, 20}

Results are reported as minimal biofilm inhibition concentration (MBIC), which is the lowest concentration inducing complete biofilm inhibition (Table 3). In addition to biofilm inhibition, the ability of the compound to disperse already established biofilms was tested at a fixed concentration of 50 μM by treating established biofilms with the compounds for 24h, followed by quantification of live attached cells as above. The monovalent glycosides D-galactose, isopropyl thiogalactoside (IPTG), **GalAG0** and **GalBG0** and dendrimers **FD2**, **GalAG2** and **GalBG2** were used as controls since their biofilm inhibition has been previously quantified using the steel coupon assay.^{5b, 12b, 13} In particular D-galactose was inactive and the monovalent glycosides were only very weakly active and showed partial biofilm inhibition or dispersal only at millimolar to molar concentrations, while **FD2**, **GalAG2** and **GalBG2** showed MBIC values of 20 μM (80 μM on a per carbohydrate basis).

G2 dendrimers **GalAxG2** and **GalBxG2** obtained by the convergent ClAc ligation approach had 2-3 fold higher MBIC values than their parent dendrimer **GalAG2** and **GalBG2**, showing a slightly detrimental effect of the modified peptide backbone on the antibiofilm activity. Nevertheless the corresponding G3 dendrimer **GalAxG3** and **GalBxG3** showed good biofilm inhibition properties with MBIC \sim 10 μM , which is comparable to the inhibition by **GalAG2** and **GalBG2** on a per galactose basis. These dendrimers were also very active in the biofilm dispersal

assay. Dendrimer **GalAxPSG4**, which was the only G4 dendrimer obtained in sufficient yields to perform biofilm inhibition studies, did not show any antibiofilm activity, however the same was true for all dendrimers with a Pro-Ser independent of their size, indicating a sequence rather than a dendrimer generation effect.

These data showed that the positive dendritic effect on biofilm inhibition in the series G0 (monovalent, no activity), G1 (divalent, weak activity for GalA only), G2 (tetravalent, strong activity in both GalA and GalB) did not extend to higher generations. Indeed the expansion to an octavalent, G3 dendrimer, although still beneficial for binding as observed in the hemagglutination and ITC experiments, did not induce a significant increase in biofilm inhibition, and expansion to G4 resulted in loss of activity. These data clearly marked tetravalency of G2 dendrimers as the optimal multivalency in this system. Although this pattern paralleled that of the relative binding potency to LecA in these series, the lack of biofilm inhibition activity with dendrimers built around a Pro-Ser core despite of their strong LecA binding showed that strong, multivalent LecA binding was necessary but not sufficient for biofilm inhibition.

Table 3. Biofilm inhibition data.

Compound	$n_{\text{gal}}^{\text{a}}$	MBIC ^(a)	MBIC $\times n_{\text{Gal}}^{\text{b}}$	Biofilm dispersal ^(c)
D-Galactose	1	> 450 mM	-	Inactive (100 mM)
IPTG	1	> 360 mM	-	25% (100 mM)
FD2	4	20 μM	80 μM	100%
GalAG0	1	> 3 mM	-	25% (0.5 mM)
GalAG1	2	225 μM	450 μM	n.d.
GalAG2	4	20 μM	80 μM	50%
GalAxG2	4	40 μM	160 μM	inactive
GalAxG3	8	9 μM	72 μM	100%
GalAxG4	16	n.d.	n.d.	n.d.
GalAPSG2	4	> 45 μM	> 180 μM	n.d.
GalAxPSG3	8	> 45 μM	> 360 μM	n.d.
GalAxPSG4	16	> 45 μM	> 720 μM	45%
GalBG0	1	> 1.35 mM	> 2.6 mM	inactive (0.25 mM)
GalBG1	2	n.d.	n.d.	n.d.
GalBG2	4	20 μM	80 μM	60%
GalBxG2	4	60 μM	240 μM	inactive
GalBxG3	8	13 μM	104 μM	100%

^{a)} MBIC: minimal biofilm inhibition concentration. ^{b)} MBIC corrected for the number of galactosyl groups. ^{c)} biofilm dispersal with 50 μM ligand.

X-ray crystallography and molecular modeling

The fact that the relative binding potency and biofilm inhibition per galactosyl group does not increase strongly beyond G2 dendrimers might reflect a steric crowding effect preventing optimal interaction with LecA at the level of G3 and G4 dendrimers. However the percentage of bound galactosyl groups deduced from ITC data indicated that essentially all galactosyl group of G2 and G3 dendrimers were bound to LecA (> 80% bound galactose), while incomplete binding only occurred at the level of the **GalAxPSG4** (40 % bound galactose). A crystallography and modelling study was therefore undertaken to propose a binding mode for the octavalent G3 dendrimers capable for accounting for the complete saturation of all eight galactosyl groups on the side of the G3 dendrimers and all four galactose binding sites on the side of lectin LecA.

After screening several complexes and conditions, good quality crystals of the complex **GalAxPSG3.LecA** were obtained by soaking crystals of LecA with the dendrimer, providing a structure at 1.9 Å resolution. In this structure LecA tetramers are arranged in a 3D checker-board lattice leaving large cavities available facing the galactose binding sites and which can be occupied by a macromolecular ligand (Figure 2A). All galactose binding sites are indeed occupied by a phenyl-β-galactosyl ligand, which under the conditions used for crystallization must be part of the terminal arms of **GalAxPSG3**. The binding interactions at the level of the phenyl-β-galactosyl groups comprise all the interactions observed previously in other aromatic galactoside LecA complexes, including hydrogen-bonding interaction between several hydroxyl groups on galactose and residues H50, D100 and N107 on LecA, as well as the critical CH-π interaction between the C(ε)-H of His50 of LecA and the aromatic group of the phenyl galactoside (Figure 2B).

No electron density is visible beyond the aromatic groups, indicating a disordered conformation of the dendrimer or a mixture of different bound states. The surface of LecA surrounding the galactose binding sites is almost entirely covered by crystal water molecules, implying **GalAxG3PS** binds LecA exclusively via its phenyl-galactosyl groups and the visible

binding interactions. The positive dendritic effect on binding affinity observed with **GalAxG3PS** and other G2 and G3 dendrimers in both hemagglutination and ITC (Table 3) can therefore only be understood in terms of a chelate binding mode in which two arms of the dendrimer bind to a pair of galactose binding site on the same side of the LecA tetramer. In the context of the crystal structure the space available in the checkboard lattice of the crystal is in any case large enough to accommodate **GalAxG3PS**.

To test if chelate-bound structures might be possible we ran independent molecular dynamics (MD) simulations of LecA (as the tetramer) in complex with **GalAxG3** and **GalAxPSG3** in a geometry compatible with the observed crystal structure. These complexes remained stable over more than 5ns of MD simulations. In particular, the protein tetramer structure retained the initial conformation seen in the X-ray model, with a global C α RMSD oscillating around 1.4 Å. Sampled structures show how the dendrimer core can arrange into a rather compact molten globule-like state, while single branches stretch out to accommodate their ends into the binding pockets of the two LecA subunits (Figure 2C). The **GalAxPSG3** dendrimer presents a more compact structure than **GalAxG3** due to the large number of more rigid proline residues (Figure 2D).

The above modeling studies suggest that G3 dendrimers bind LecA in a chelate bound mode with a pair of galactosyl groups combining with a pair of galactose binding sites on the same side of LecA. G3 dendrimers are clearly too small to bridge between two pairs of galactose binding sites on opposite sides of the same tetramer. The crystal structure of the **GalAxPSG3**.LecA complex most likely corresponds to a 2:1 dendrimer/LecA tetramer stoichiometry engaging only a single pair of galactosyl groups per dendrimer (Figure 2E). ITC data by contrast show that all galactoside groups engage in a binding interaction with LecA, which can only occur with the opposite 1:2 dendrimer/LecA stoichiometry. Such stoichiometry might occur in a cross-linked network accounting for the formation of precipitates during ITC with all higher generation dendrimers (Figure 2F).

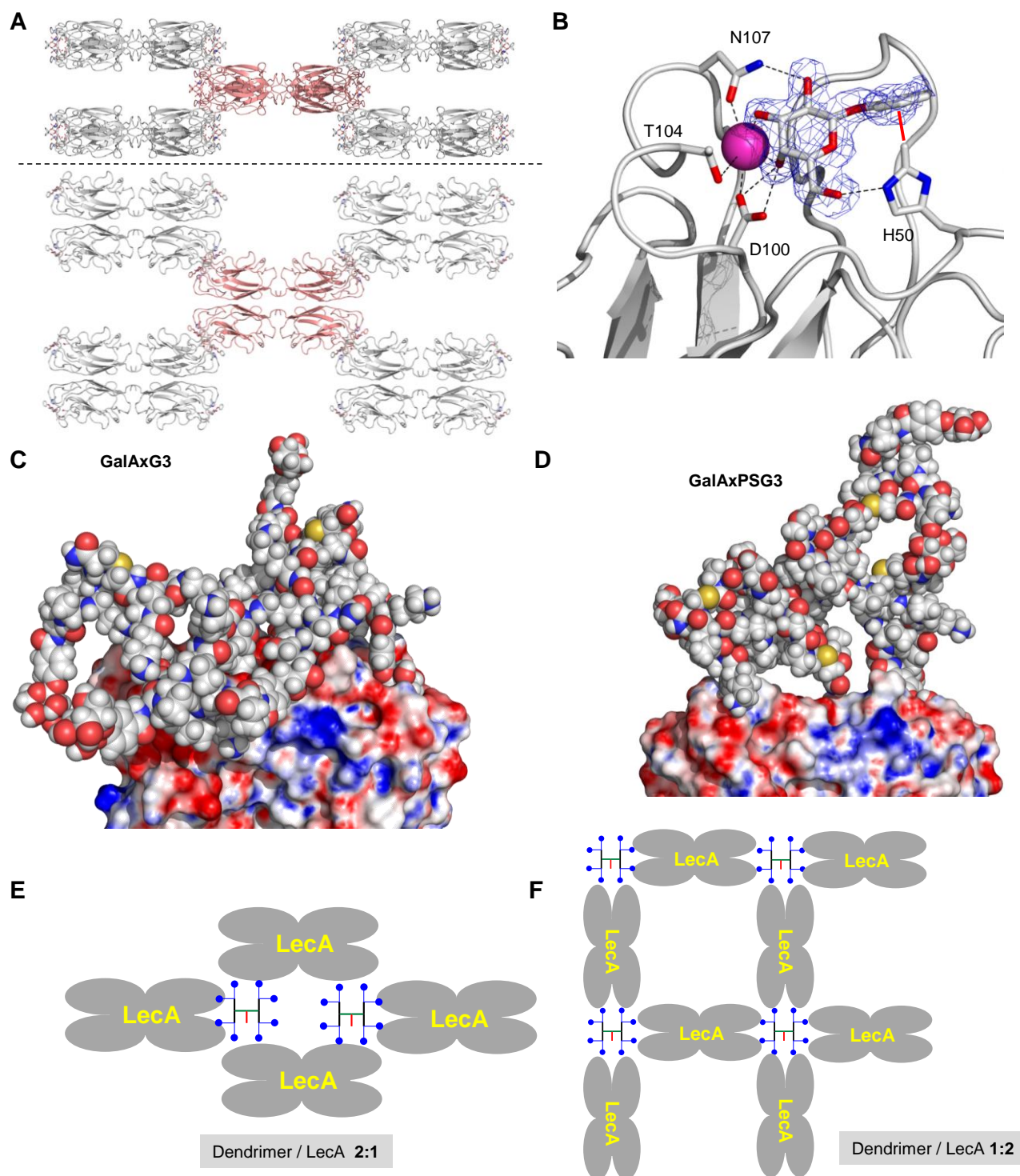


Figure 2. Crystal structure and molecular modeling of G3 dendrimer LecA interactions. **A.** Side view and top view of the 3D checker-board lattice of the **GalAxPSG3.LecA** complex in the crystal (PDB 5D21). One LecA tetramer (red) is shown surrounded by its eight neighbours making contact at each of the eight corners. **B.** Details of the visible electron density of **GalAxPSG3** and dendrimer-lectin binding interactions. **C.** Snapshot of the MD simulation of a chelate bound **GalAxG3.LecA** complex. **D.** Snapshot of a chelate bound **GalAxPSG3.LecA** complex. **E.** Schematic representation of LecA crystal lattice bound to a G3 dendrimer. **F.** Schematic representation of an extensive G3 dendrimer.LecA lattice accounting for saturation of all galactosyl groups and galactose binding sites.

Conclusion

In summary, convergent synthesis using the ClAc ligation as key step enabled an efficient synthesis of G3 and G4 glycopeptide dendrimer ligands for the galactose specific *P. aeruginosa* lectin LecA bearing either 4-carboxyphenyl- β -galactoside (GalA) or carboxypropyl- β -thiogalactoside (GalB) end groups. LecA complexation studies by hemagglutination assay and by ITC showed that the strong positive effect on relative binding affinity per galactosyl group observed up to the tetravalent G2 dendrimers only partially extended to the octavalent G3 dendrimers, and that G4 dendrimers had decreased relative binding affinities. Similar effects were observed in *P. aeruginosa* biofilm inhibition and dispersal assays, with dendrimers **GalAxG3** and **GalBxG3** showing comparable activities to G2 dendrimers in biofilm inhibition and slightly better activities in biofilm dispersal. A crystal structure and modeling study was used to propose a lattice binding model accounting for the saturation of all dendrimer galactosyl groups and LecA galactose binding site for these potent G3 dendrimers. Further studies with additional glycopeptide dendrimers diversified using the efficient ClAc ligation approach are underway to decipher the structure-activity relationships in this system in more detail and will be reported in due course.

Materials and Methods

Synthesis

Amino acids were used as the following derivatives: Fmoc-His(Trt)-OH, Fmoc-Leu-OH, Fmoc-Phe-OH, Fmoc-Ile-OH, Fmoc-Pro-OH, Fmoc-Lys(Boc)-OH, Fmoc-Lys(Fmoc)-OH, Fmoc-Cys(Trt)-OH, Fmoc-Ser(tBu)-OH. Chemicals were used as supplied and solvents were of analytical grade. Analytical RP-UHPLC was performed in Dionex ULTIMATE 3000 RS chromatography system (ULTIMATE 3000 RS Photo diode array detector) using a Dionex Acclaim® RSLC 120

C18, 3.0 x 50 mm, particle size 2.2 μm , 120 \AA pore size, flow rate 1.2 ml min⁻¹ column. Eluent A contained water with 0.1% TFA; eluent D contained acetonitrile and water (90:10) with 0.1% TFA. Compounds were detected by UV absorption at 214 nm. Preparative RP-HPLC was performed with HPLC-grade acetonitrile and MilliQ deionized water using a Dr. Maisch GmbH Reprospher C18-DE, 100 x 30 mm, particle size 5 μm , 100 \AA pore size column installed on a Waters Prep LC Controller system (flow rate 40 ml min⁻¹). Eluent A contained water with 0.1% TFA; eluent B contained acetonitrile and water (60:40) with 0.1% TFA. MS spectra were provided by the Service of Mass Spectrometry of the Department of Chemistry and Biochemistry, University of Bern.

Solid phase peptide synthesis. Dendrimers were synthesized on solid phase using Fmoc chemistry in a plastic syringes (10 mL) mounted on the axis of a rotatory agitator for gentle stirring during reactions.²¹ Rink amide NovaSyn® TGR resin (loading: 0.23 mmol/g) (purchased from Novabiochem) was acylated with each Fmoc-protected α -amino acid (3 eq) in the presence of benzotriazol-1-yl-oxytripyrrolidinophosphonium hexafluorophosphate (PyBOP) (3 eq) and *N,N*-Diisopropylethylamine (DIEA) (5 eq) in *N*-Methyl-2-pyrrolidone (NMP). The Fmoc-protecting groups were removed with a solution of 20% piperidine in DMF. When necessary the resin was chloroacetylated twice with a solution of chloroacetic acid anhydride (10 eq) in NMP for 20 min. In the end of the other sequences the terminal amino acids were coupled with the protected sugar derivative (5 eq) in the presence of DIEA (5 eq) and 2-(6-Chloro-1H-benzotriazole-1-yl)-1,1,3,3-tetramethylaminium hexafluorophosphate) (HCTU) (3 eq). The carbohydrate was deprotected with a solution of MeOH/NH₃/H₂O (v/v 8:1:1). The resin was dried and the cleavage was carried out with TFA/ Triisopropylsilane/H₂O (95:2.5:2.5). Peptide dendrimers containing Cys residues were cleaved with TFA/Triisopropylsilane/H₂O/1,2-ethanedithiol (94:1:2.5:2.5). Peptide dendrimers were precipitated with methyl *tert*-butyl ether and purified by preparative HPLC. The compounds **GalAG0**, **GalAG1**, **GalAG2**, **GalBG0**, **GalBG1** and **GalBG2** were prepared as previously described.¹³

Thioether ligation. A solution of core dendrimer (sequence containing chloroacetyl endgroups, around 3 mg, 1 eq) and KI (20 eq) in DMF/H₂O (1:1, v/v) (300 ul) was prepared in a 2 mL glass vial. The mixture was degassed with Ar during 10 min. In another 2 mL glass vial arm dendrimer (Cys containing sequence, 1.5 eq per chloroacetyl endgroup in core sequence) was weighed and degassed with Ar during 10 min. The core dendrimer/KI solution was transferred to the glass vial containing the arm dendrimer via a gas-tight syringe. DIEA (55 eq) was added and the solution stirred overnight at room temperature under Ar atmosphere. The reaction was followed by analytical RP-UHPLC. After 16 to 23 h, the reaction was quenched by the addition of 3.5 mL of eluent A. After filtration, the solution was directly purified by preparative RP-HPLC.

GalAG1-Cys (GalA-KP)₂KIC was obtained from 500 mg resin (loading 0.22 mmol · g⁻¹) as a foamy white solid after preparative RP-HPLC (63 mg, 45.76 μmol, 42%). Analytical RP-UHPLC: t_R = 1.257 min (A/D 100/0 to 0/100 in 2.2 min, λ = 214 nm). MS (ESI+) calc for C₆₃H₉₇N₁₁O₂₁S [M+H]⁺: 1376.6, found 1376.6, [M+H]⁺/2 688.6

GalBG1-Cys (GalB-KP)₂KIC was obtained from 500 mg resin (loading 0.22 mmol · g⁻¹) as a foamy white solid after preparative RP-HPLC (57 mg, 43.43 μmol, 40%). Analytical RP-UHPLC: t_R = 1.217 min (A/D 100/0 to 0/100 in 2.2 min, λ = 214 nm). MS (ESI+) calc for C₅₅H₉₇N₁₁O₁₉S₃ [M+H]⁺: 1312.6, found 1312, [M+H]⁺/2 656.8

CIacG1 (CIac-KI)₂KHI was obtained from 500 mg resin (loading 0.22 mmol · g⁻¹) as a foamy white solid after preparative RP-HPLC (41.4 mg, 40.18 μmol, 33%). Analytical RP-UHPLC: t_R = 0.990 min (A/D 80/20 to 0/100 in 2.2 min, λ = 214 nm). MS (ESI+) calc for C₄₆H₈₁Cl₂N₁₃O₉ [M+H]⁺: 1031.1, found 1030.4, [M+H]⁺/2 515.8; [M+H]⁺/3 344.6

CIacG2 (CIac-KP)₄(KKI)₂KHI was obtained from 500 mg resin (loading 0.22 mmol · g⁻¹) as a foamy white solid after preparative RP-HPLC (64 mg, 27.34 μmol, 25%). Analytical RP-UHPLC: t_R = 1.345 min (A/D 100/0 to 0/100 in 2.2 min, λ = 214 nm). MS (ESI+) calc for C₁₀₆H₁₈₃Cl₄N₂₉O₂₁ [M+H]⁺: 2341.6, found 2341.0.

CIAcG3 (CIAc-KP)₈(KLF)₄(KKI)₂KHI was obtained from 500 mg resin (loading 0.25 mmol · g⁻¹) as a foamy white solid after preparative RP-HPLC (19.3 mg, 3.78 μmol, 3%). Analytical RP-UHPLC: t_R = 1.647 min (A/D 100/0 to 0/100 in 2.2 min, λ = 214 nm). MS (ESI+) calc for C₂₄₂H₃₉₁Cl₈N₅₇O₄₅ [M+H]⁺: 5102.7, found 5102.

CIAcPSG2 (CIAc-PS)₄(KPS)₂KPS was obtained from 500 mg resin (loading 0.22 mmol · g⁻¹) as a foamy white solid after preparative RP-HPLC (66 mg, 33.07 μmol, 30%). Analytical RP-UHPLC: t_R = 1.285 min (A/D 90/10 to 0/100 in 2.2 min, λ = 214 nm). MS (ESI+) calc for C₈₂H₁₂₇Cl₄N₂₁O₂₈ [M+H]⁺: 1996.8, found 1995.9, 2033.9 [M+K]⁺, 2056.4 [M+K+Na]⁺

CIAcPSG3 (CIAc-PS)₈(KPS)₄(KPS)₂KPS was obtained from 500 mg resin (loading 0.22 mmol · g⁻¹) as a foamy white solid after preparative RP-HPLC (25 mg, 5.83 μmol, 5%). Analytical RP-UHPLC: t_R = 1.38 min (A/D 90/10 to 0/100 in 2.2 min, λ = 214 nm). MS (ESI+) calc for C₁₇₈H₂₇₅Cl₈N₄₅O₆₀ [M+H]⁺: 4289, found 4290 and several sodium and potassium adducts.

GalAPSG2 (GalA-KPL)₄(KPS)₂KPS was obtained from 500 mg resin (loading 0.25 mmol · g⁻¹) as a foamy white solid after preparative RP-HPLC (26.4 mg, 7.68 μmol, 6%). Analytical RP-UHPLC: t_R = 2.635 min (A/D 100/0 to 0/100 in 7.5 min, λ = 214 nm). MS (ESI+) calc for C₁₆₂H₂₅₁N₂₉O₅₂ [M+H]⁺: 3437.89, found 3437.8. Calc. for [M+K]⁺ : 3475.89, found 3975.7.

GalAxG2 (GalA-KP)₄(KICxKI)₂KHI was obtained as a foamy white solid after preparative RP-HPLC (6.9 mg, 1.86 μmol, 68%). Analytical RP-UHPLC: t_R = 1.944 min (A/D 100/0 to 0/100 in 4.5 min, λ = 214 nm). MS (ESI+) calc for C₁₇₂H₂₇₃N₃₅O₅₁S₂ [M+H]⁺: 3711.3, found 3711.0.

GalAxG3 (GalA-KP)₈(KICxKP)₄(KKI)₂KHI was obtained as a foamy white solid after preparative RP-HPLC (6.6 mg, 0.86 μmol, 67%). Analytical RP-UHPLC: t_R = 1.799 min (A/D 100/0 to 0/100 in 4.5 min, λ = 214 nm). MS (ESI+) calc for C₃₅₈H₅₆₇N₇₃O₁₀₅S₄ [M+H]⁺: 7702, found 7701.0; [M+H]⁺ adducts with trifluoroacetic acid (TFA)

GalAxG4 (GalA-KP)₁₆(KICxKP)₈(KLF)₄(KKI)₂KHI was obtained as a foamy white solid after preparative RP-HPLC (1.1 mg, 0.07 μ mol, 12%). Analytical RP-UHPLC: t_R = 2.094 min (A/D 100/0 to 0/100 in 4.5 min, λ = 214 nm). MS (ESI+) calc for C₇₄₆H₁₁₅₉N₁₄₅O₂₁₃S₈ [M+H]⁺: 15'824, found 15'825.

GalAxPSG3 (GalA-KP)₈(KICxPS)₄(KPS)₂KPS was obtained as a foamy white solid after preparative RP-HPLC (8.2 mg, 1.11 μ mol, 74%). Analytical RP-UHPLC: t_R = 2.519 min (A/D 100/0 to 0/100 in 7.5 min, λ = 214 nm). MS (ESI+) calc for C₃₃₄H₅₁₁N₆₅O₁₁₂S₄ [M+H]⁺: 7357.3, found 7358.0, [M+K]⁺ 7395.0

GalAxPSG4 (GalA-KP)₁₆(KICxPS)₈(KPS)₄(KPS)₂KPS was obtained as a foamy white solid after preparative RP-HPLC (9.1 mg, 0.61 μ mol, 81%). Analytical RP-UHPLC: t_R = 1.878 min (A/D 100/0 to 0/100 in 4.5 min, λ = 214 nm). MS (ESI+) calc for C₆₈₂H₁₀₄₃N₁₃₃O₂₂₈S₈ [M+H]⁺: 15'010, found 15'010.3.

GalBxG2 (GalB-KP)₄(KICxKI)₂KHI was obtained as a foamy white solid after preparative RP-HPLC (5.2 mg, 1.45 μ mol, 50%). Analytical RP-UHPLC: t_R = 1.839 min (A/D 100/0 to 0/100 in 4.5 min, λ = 214 nm). HRMS (ESI+) calc for C₁₅₆H₂₇₃N₃₅O₄₇S₆ [M+H]⁺: 3583.4, found 3582.84.

GalBxG3 (GalB-KP)₈(KICxKP)₄(KKI)₂KHI was obtained as a foamy white solid after preparative RP-HPLC (4.9 mg, 0.66 μ mol, 51%). Analytical RP-UHPLC: t_R = 1.784 min (A/D 100/0 to 0/100 in 4.5 min, λ = 214 nm). MS (ESI+) calc for C₃₂₆H₅₆₇N₇₃O₉₇S₁₂ [M+H]⁺: 7446, found 7445.0

Hemagglutination Assays

A) Erythrocytes preparation. Rabbit red cells (erythrocytes 50%; Biomerieux) separated from preservative by centrifugation (1500 RPM; 10min), were washed three times with 0.9% NaCl solution (saline) and suspended to a concentration of 5% v/v in phosphate buffer saline (PBS; 0.01 M; pH 7.4). The suspension was given papain-treatment which includes incubation of 9 volumes of the 5% cell suspension with 1 volume of the 1% w/v papain (crude preparation, Sigma) in 0.1% w/v

L-cysteine solution at 37° for 30 min. The enzyme treated cells were washed three times in PBS and then resuspended in it to a concentration of 5%.

B) LecA titration. In order to determine the lectin concentration needed to agglutinate the cells, decreasing amounts of LecA were incubated with red blood cells. Serial two fold dilutions were made in the wells of microtiter plate (96-well microtiter non-treated V-bottom plates, Nunc, Denmark). The two fold dilutions were made by adding 50 μ L of buffer solution to the all 24 wells and 50 μ L of LecA solution (0.34 mg/ml) to the first well. 50 μ L was then transferred from the first well to the second. The second well was mixed and 50 μ L was transferred to the third well. This procedure was repeated until the 24th well. To each well 50 μ L of the RBCs solution (5% in PBS) was added and incubated for 30 min at 4°C. After this time, plates were centrifuged for 30s (1,000 x g), the wells were examined and the minimum amount of LecA required to agglutinate the cell suspension was determined. This was then considered to be 1 HA unit. For the inhibition assay an 8 HA unit LecA solution was made up.

C) Minimum Inhibitory Concentration (MIC) determination. A 50 μ L sample of each inhibitor examined was serially diluted with 50 μ L PBS in the microtiter plate to produce twofold dilutions (as described above). The inhibitor solutions were incubated with 50 μ L of the 8 HA unit LecA solution (Conc. of LecA = 5.31 μ g/mL) for 30 min at 4°C. After this time 50 μ L of the erythrocytes in PBS suspensions (Conc.5%) was added and the wells were mixed and incubated for one hour in the room temperature. The plates were then centrifuged for 30s (1,000 x g). Each test was performed in triplicate. The activity of the tested compounds was recorded as minimal inhibitory concentration (MIC), corresponding to the highest dilution causing a complete inhibition of hemagglutination (Supporting information Figure S46).

Isothermal Titration Calorimetry (ITC)

Lyophilized LecA was dissolved in buffer (Tris 20 mM, NaCl 100 mM, CaCl₂ 100 μM, pH=7.5). Protein concentration was checked by measurement of absorbance at 280 nm using 1 Abs = 2.116 mg/ml (M_w = 12'893 g/mol) using a NanoDrop instrument. Ligands were dissolved directly into the same buffer. ITC was performed with iTC₂₀₀ calorimeter (MicroCal Inc.). Titration was performed on 0.0146-0.3 mM LecA in the 200 μl sample cell using 2 μl injections of 0.01-01 mM ligand every 120s at 25 °C. The data were fitted with MicroCal Origin 8 software, according to standard procedures using a single-site model. Change in free energy ΔG was calculated from the equation: $\Delta G = \Delta H - T\Delta S$ where T is the absolute temperature, ΔH and ΔS are the change in enthalpy and entropy respectively. Two independent titrations were performed for each ligand tested.

Biofilm inhibition

A modified version of the method described by Diggle et al. was employed.^{5b} 96-well sterile, U-bottomed polystyrene microtitre plates (TPP Switzerland) were prepared by adding 200 μl of sterile deionized water to the peripheral wells to decrease evaporation from test wells. Aliquots of 180 μl of culture medium (10% (w/v) nutrient broth No. 2, Oxoid) containing desired concentration of the test compound were added to the internal wells. Inoculum of *P. aeruginosa* strain PAO1 was prepared from 5 ml overnight culture grown in LB broth. Aliquots of 20 μl of overnight cultures, pre-washed in 10% (w/v) nutrient broth and normalized to an OD₆₀₀ of 1, were inoculated into the test wells. Plates were incubated in a humid environment for 25 hours at 37°C. Wells were washed with 200 μl sterile deionized water before staining with 200 μl 10% (w/v) nutrient broth containing 0.5 mM WST-8 and 20 μM phenazine ethosulfate for 3 hours at 37°C. Afterwards, the well supernatants were transferred to a polystyrene flat bottomed 96-well plate (TPP Switzerland) and the absorbance was measured at 450 nm with a plate reader (SpectraMax250 from Molecular Devices).

Crystallization of GalAxPSG3.LecA

LecA was expressed and purified by affinity chromatography along an optimized protocol and in accordance to a previous report.¹⁷ The crystals of the **GalAxPSG3.LecA** complex were obtained by soaking. For this, LecA crystals were grown in a condition containing 1.5M ammonium sulfate at a pH of 4.6 which is the SaltRx II 13 condition. The crystals grew within 3-4 days. Drops of 4 μ L containing the crystals were supplemented with GalAPSG3 at 15 binding equivalents of compound, respectively. The soaked crystals were incubated at 18 °C for 3-4 days, transferred into a solution of 1.5M ammonium sulfate supplemented with 30 % v/v glycerol at pH 4.6 and immediately flash frozen in liquid nitrogen for storage. Further details on data collection statistics are given in (Table S1). Crystals were cryo cooled at 100 K after soaking them for as short a time as possible in glycerol 30% v/v in precipitant solution. All data were collected at the SLS synchrotron (Villigen, Switzerland) at beamline PX-II/III. The structures were solved with CCP4 and Phenix.^{22,23}

Molecular modeling

The crystal structure of **GalAxPSG3.LecA** obtained above was used to model the dendrimer.LecA complexes. Two systems were considered: (i) LecA in complex with **GalAxG3** and (ii) LecA in complex with **GalAxPSG3**. The initial configurations were built using Corina,²⁴ imposing binding two units of GalA in two binding pocket of the respective LecA subunits. The missing hydrogen atoms were added to the protein structure using the default protonation states at pH=7. The amber force field (FF99SB)²⁵ was used to describe intra- and inter-molecular interactions. The electrostatic point-charges for the GalA unit, and for the branching lysine and modified cysteine amino acids present in the dendrimer structures were obtained using the standard RESP procedure.²⁶ The **GalAxPSG3.LecA** and **GalAxG3.LecA** systems were solvated by 60531 and 71608 water molecules and placed in a truncated octahedral water box. The TIP3P water model²⁷ was used to add solvent. Particle Mesh Ewald routines were used to treat long-range electrostatic interactions.²⁸ A cutoff of 11 Å was used for the van der Waals interactions and the real part of the electrostatic

potential. The simulations were performed using Langevin dynamics for temperature regulation²⁹ Bonds comprising hydrogen atoms were constrained with the SHAKE constraint algorithm³⁰ All simulations were performed using the AMBER12³¹ program and the trajectories were analyzed using VMD.³² First, energy minimization on the entire system was carried out using the steepest descent algorithm for the first 1000 steps followed by 2500 steps of conjugate gradient algorithm. The solvent was then heated up from 0 to 300 K in 200 ps MD, using a time step of 2fs. This step assigns weak positional restraints on the solute. After this procedure the whole system was energy minimized. Finally production runs of 5 ns were performed at 300 K.

Acknowledgements. This work was supported financially by the University of Bern, the Swiss National Science Foundation, and the COST Actions D34 and CM1102 MultiGlycoNano. We thank the staff at the Swiss Light Source, Beamline X06DA (PXIII), Villigen, Switzerland, for support during data collection.

References

1. V. E. Wagner and B. H. Iglewski, *Clin. Rev. Allergy Immunol.*, 2008, **35**, 124-134.
2. a) M. N. Hurley, M. Camara and A. R. Smyth, *Eur. Respir. J.*, 2012, **40**, 1014-1023; b) J. Valle, S. Da Re, N. Henry, T. Fontaine, D. Balestrino, P. Latour-Lambert and J. M. Ghigo, *Proc. Natl. Acad. Sci. U. S. A.*, 2006, **103**, 12558-12563.
3. a) N. Garber, U. Guempel, A. Belz, N. Gilboa-Garber and R. J. Doyle, *Biochim. Biophys. Acta*, 1992, **1116**, 331-333; b) G. Cioci, E. P. Mitchell, C. Gautier, M. Wimmerova, D. Sudakevitz, S. Perez, N. Gilboa-Garber and A. Imberty, *FEBS Lett*, 2003, **555**, 297-301; c) A. Imberty, M. wimmerova, E. P. Mitchell and N. Gilboa-Garber, *Microbes Infect.*, 2004, **6**, 221-228.
4. a) E. Mitchell, C. Houles, D. Sudakevitz, M. Wimmerova, C. Gautier, S. Perez, A. M. Wu, N. Gilboa-Garber and A. Imberty, *Nat. Struct. Biol.*, 2002, **9**, 918-921; b) R. Loris, D. Tielker, K. E. Jaeger and L. Wyns, *J. Mol. Biol.*, 2003, **331**, 861-870.
5. a) M. Mewe, D. Tielker, R. Schonberg, M. Schachner, K. E. Jaeger and U. Schumacher, *J. Laryngol. Otol.*, 2005, **119**, 595-599; b) S. P. Diggle, R. E. Stacey, C. Dodd, M. Camara, P. Williams and K. Winzer, *Environ. Microbiol.*, 2006, **8**, 1095-1104.
6. a) H. P. Hauber, M. Schulz, A. Pforte, D. Mack, P. Zabel and U. Schumacher, *Int. J. Med. Sci.*, 2008, **5**, 371-376; b) C. Chemani, A. Imberty, S. de Bentzmann, M. Pierre, M. Wimmerova, B. P. Guery and K. Faure, *Infect. Immun.*, 2009, **77**, 2065-2075.

7. A. Bernardi, J. Jimenez-Barbero, A. Casnati, C. De Castro, T. Darbre, F. Fieschi, J. Finne, H. Funken, K. E. Jaeger, M. Lahmann, T. K. Lindhorst, M. Marradi, P. Messner, A. Molinaro, P. V. Murphy, C. Nativi, S. Oscarson, S. Penades, F. Peri, R. J. Pieters, O. Renaudet, J. L. Reymond, B. Richichi, J. Rojo, F. Sansone, C. Schaffer, W. B. Turnbull, T. Velasco-Torrijos, S. Vidal, S. Vincent, T. Wennekes, H. Zuilhof and A. Imberty, *Chem. Soc. Rev.*, 2013, **42**, 4709-4727.
8. S. Cecioni, A. Imberty and S. Vidal, *Chem. Rev.*, 2015, **115**, 525-561.
9. B. Gerland, A. Goudot, G. Pourceau, A. Meyer, S. Vidal, E. Souteyrand, J. J. Vasseur, Y. Chevolot and F. Morvan, *J. Org. Chem.*, 2012, **77**, 7620-7626.
10. a) A. Imberty, Y. M. Chabre and R. Roy, *Chem. Eur. J.*, 2008, **14**, 7490-7499; b) R. J. Pieters, *Org. Biomol. Chem.*, 2009, **7**, 2013-2025; c) V. Wittmann and R. J. Pieters, *Chem. Soc. Rev.*, 2013, **42**, 4492-4503.
11. G. M. L. Consoli, G. Granata, V. Cafiso, S. Stefani and C. Geraci, *Tetrahedron Lett.*, 2011, **52**, 5831-5834.
12. a) E. M. V. Johansson, E. Kolomiets, F. Rosenau, K.-E. Jaeger, T. Darbre and J.-L. Reymond, *New J. Chem.*, 2007, **31**, 1291-1299; b) E. M. Johansson, S. A. Crusz, E. Kolomiets, L. Buts, R. U. Kadam, M. Cacciarini, K. M. Bartels, S. P. Diggle, M. Camara, P. Williams, R. Loris, C. Nativi, F. Rosenau, K. E. Jaeger, T. Darbre and J. L. Reymond, *Chem. Biol.*, 2008, **15**, 1249-1257; c) E. Kolomiets, M. A. Swiderska, R. U. Kadam, E. M. Johansson, K. E. Jaeger, T. Darbre and J. L. Reymond, *ChemMedChem*, 2009, **4**, 562-569; d) E. M. V. Johansson, R. U. Kadam, G. Rispoli, S. A. Crusz, K.-M. Bartels, S. P. Diggle, M. Camara, P. Williams, K.-E. Jaeger, T. Darbre and J.-L. Reymond, *MedChemComm*, 2011, **2**, 418-420.
13. R. U. Kadam, M. Bergmann, M. Hurley, D. Garg, M. Cacciarini, M. A. Swiderska, C. Nativi, M. Sattler, A. R. Smyth, P. Williams, M. Camara, A. Stocker, T. Darbre and J. L. Reymond, *Angew. Chem., Int. Ed.*, 2011, **50**, 10631-10635.
14. a) T. Darbre and J. L. Reymond, *Curr. Top. Med. Chem.*, 2008, **8**, 1286-1293; b) J.-L. Reymond and T. Darbre, *Org. Biomol. Chem.*, 2012, **10**, 1483-1492; c) J. L. Reymond, M. Bergmann and T. Darbre, *Chem. Soc. Rev.*, 2013, **42**, 4814-4822.
15. C. C. Lee, J. A. MacKay, J. M. J. Frechet and F. C. Szoka, *Nature Biotechnol.*, 2005, **23**, 1517-1526.
16. R. Visini, X. Jin, M. Bergmann, G. Michaud, F. Pertici, O. Fu, A. Pukin, T. R. Branson, D. M. Thies-Weesie, J. Kemmink, E. Gillon, A. Imberty, A. Stocker, T. Darbre, R. J. Pieters and J. L. Reymond, *ACS Chem. Biol.*, 2015, ASAP.
17. R. U. Kadam, M. Bergmann, D. Garg, G. Gabrieli, A. Stocker, T. Darbre and J.-L. Reymond, *Chem. Eur. J.*, 2013, **18**, 17054-17063.
18. N. A. Uhlich, T. Darbre and J. L. Reymond, *Org. Biomol. Chem.*, 2011, **9**, 7071-7084.
19. a) N. W. Roehm, G. H. Rodgers, S. M. Hatfield and A. L. Glasebrook, *J Immunol Methods*, 1991, **142**, 257-265; b) E. Peeters, H. J. Nelis and T. Coenye, *J. Microbiol. Methods*, 2008, **72**, 157-165; c) S. Stepanovic, D. Vukovic, V. Hola, G. Di Bonaventura, S. Djukic, I. Cirkovic and F. Ruzicka, *APMIS*, 2007, **115**, 891-899; d) M. Ishiyama, Y. Miyazono, K. Sasamoto, Y. Ohkura and K. Ueno, *Talanta*, 1997, **44**, 1299-1305.

20. B. Adam, G. S. Baillie and L. J. Douglas, *J. Med. Microbiol.*, 2002, **51**, 344-349.
21. N. Maillard, A. Clouet, T. Darbre and J. L. Reymond, *Nat. Protoc.*, 2009, **4**, 132-142.
22. M. D. Winn, C. C. Ballard, K. D. Cowtan, E. J. Dodson, P. Emsley, P. R. Evans, R. M. Keegan, E. B. Krissinel, A. G. W. Leslie, A. McCoy, S. J. McNicholas, G. N. Murshudov, N. S. Pannu, E. A. Potterton, H. R. Powell, R. J. Read, A. Vagin and K. S. Wilson, *Acta Cryst.*, 2011, **67**, 235-242.
23. P. D. Adams, P. V. Afonine, G. Bunkoczi, V. B. Chen, I. W. Davis, N. Echols, J. J. Headd, L.-W. Hung, G. J. Kapral, R. W. Grosse-Kunstleve, A. J. McCoy, N. W. Moriarty, R. Oeffner, R. J. Read, D. C. Richardson, J. S. Richardson, T. C. Terwilliger and P. H. Zwart, *Acta Cryst.*, 2010, **66**, 213-221.
24. J. Sadowski, J. Gasteiger and G. Klebe, *J. Chem. Inf. Comput. Sci.*, 1994, **34**, 1000-1008.
25. V. Hornak, R. Abel, A. Okur, B. Strockbine, A. Roitberg and C. Simmerling, *Proteins*, 2006, **65**, 712-725.
26. C. I. Bayly, P. Cieplak, W. Cornell and P. A. Kollman, *J. Phys. Chem.*, 1993, **97**, 10269-10280.
27. W. L. Jorgensen, J. Chandrasekhar, J. D. Madura, R. W. Impey and M. L. Klein, *J. Chem. Phys.*, 1983, **79**, 926-935.
28. a) T. Darden, D. York and L. Pedersen, *J. Chem. Phys.*, 1993, **98**, 10089-10092; b) U. Essmann, L. Perera, M. L. Berkowitz, T. Darden, H. Lee and L. G. Pedersen, *J. Chem. Phys.*, 1995, **103**, 8577-8593.
29. D. S. Cerutti, R. Duke, P. L. Freddolino, H. Fan and T. P. Lybrand, *J. Chem. Theory Comput.*, 2008, **4**, 1669-1680.
30. J. P. Ryckaert, G. Ciccotti and H. J. C. Berendsen, *J. Comput. Phys.*, 1977, **23**, 327-341.
31. J. C. Phillips, R. Braun, W. Wang, J. Gumbart, E. Tajkhorshid, E. Villa, C. Chipot, R. D. Skeel, L. Kalé and K. Schulten, *J. Comput. Chem.*, 2005, **26**, 1781-1802.
32. B. Hess, C. Kutzner, D. van der Spoel and E. Lindahl, *J. Chem. Theory Comput.*, 2008, **4**, 435-447.

Table of Contents Graphics :

